Diversity-oriented synthesis as a tool for identifying new modulators of mitosis

Brett M. Ibbeson[1,*], Luca Laraia[1,2,*], Esther Alza[1], Cornelius J. O' Connor[1], Yaw Sing Tan[1], Huw M. L. Davies[3], Grahame McKenzie[2], Ashok R. Venkitaraman[2], David R. Spring[1]

[1]Department of Chemistry, University of Cambridge, Cambridge, UK, CB2 1EW. [2] MRC Cancer Unit, University of Cambridge, Hutchison/MRC Research Centre, Box 197, Biomedical Campus, Cambridge, UK, CB2 0XZ. [3]Department of Chemistry, Emory University, 440 Atwood Hall, 1515 Dickey Drive, Atlanta GA 30322. [*]Authors contributed equally to this work. Correspondance and requests for materials should be addressed to A.R.V. (e-mail arv22@hutchison-mrc.cam.ac.uk) or D.R.S. (e-mail spring@ch.cam.ac.uk)

ABSTRACT

The synthesis of diverse 3-dimensional libraries has become of paramount importance for obtaining better leads for drug discovery. Such libraries are predicted to fare better than traditional compound collections in phenotypic screens and against difficult targets. Herein we report the diversity-oriented synthesis (DOS) of a compound library using rhodium carbenoid chemistry to access structurally diverse, 3-dimensional molecules, and show that they access biologically relevant areas of chemical space using cheminformatic analysis. High content screening (HCS) of this library for anti-mitotic activity, followed by chemical modification identified 'Dosabulin', which causes mitotic arrest and cancer cell death by apoptosis. Its mechanism of action is determined to be microtubule depolymerization, and the compound is shown to not significantly affect Vinblastine binding to tubulin, however experiments suggest binding to a site vicinal or allosteric to Colchicine. This work validates the combination of DOS and phenotypic screening as a strategy for the discovery of biologically relevant chemical entities.

INTRODUCTION

Diversity-oriented synthesis (DOS) aims to synthesize libraries of structurally complex and functionally diverse small molecules in an efficient manner[1, 2]. Biomolecules interact with each other in a three dimensional environment, and consequently, functional diversity is directly associated with the three dimensional chemical information the surface of a small molecule presents when interacting with macromolecules, such as protein. The last decade has witnessed the emergence of several distinct DOS strategies for the construction of chemically diverse libraries[3-5]. One such method, the *reagent-based* approach[3], involves synthesizing one or more densely functionalized molecules, which can subsequently be transformed into diverse molecular scaffolds. These molecules can be reacted selectively with a wide variety of reagents, providing access to an array of distinct molecular frameworks. Alternatively, a single pluripotent functional group can be exploited by subjecting it to a wide variety of reaction conditions thereby enabling the synthesis of multiple molecular skeletons. Carbenoid chemistry offers exciting opportunities for DOS applications, particularly in the context of the reagent-based approach. A wealth of distinct reactions can be performed using carbenoid chemistry,[6] and its applicability to library construction, was recently exemplified by Panek and co-workers[7]. In addition to scaffold diversity, increasing carbogenic sp^3 content and the number of stereocentres has been suggested to enhance selectivity and potency for a given target, and increase hit rate across several targets from a single library[8]. Furthermore, increasing sp^3 count correlates favourably with decreasing clinical toxicity[9], and decreasing aromatic ring count is likely to produce less compound attrition in drug discovery[10]. It is important that these considerations are implemented in DOS strategies and that effective methods are developed to enable the efficient synthesis of structurally diverse compound collections.

Phenotypic screening is an expedient mechanism for identifying small molecules that perturb biological function. It provides an efficient way to evaluate the biological activity of a compound collection against a wide variety of molecular targets[11]. Recently it has also been established that the vast majority of first-in-class drugs were identified by phenotypic screening[12]. Our group and others have successfully implemented this approach in combination with DOS to discover novel small molecule modulators of biological function[13]. In 2008, we discovered gemmacin, a small molecule with similar potency to clinically used antibiotics and improved activity against resistant bacterial strains[14]. Other groups have also used this approach effectively; some notable examples include the discovery of the novel Hedgehog pathway modulator robotnikinin[15], and compounds with interesting anti-malarial properties[16]. Another related approach termed biology-oriented synthesis (BIOS), has also led to the identification of many useful tool compounds from phenotypic screens[17-19]. Phenotypic screening has been used effectively to discover new anti-mitotics[20, 21]. Whilst several clinically used anti-mitotics exist, they often suffer from administration or resistance problems[22, 23]. Additionally, they are mostly derived from natural products, making chemical modification difficult. Therefore there is an increased requirement for new compounds that cause mitotic arrest.

Herein, we report the efficient synthesis of a functionally diverse compound collection, using rhodium carbenoid chemistry in a reagent-based approach. These molecules display a high sp^3 content and access biologically relevant areas of chemical space. Furthermore, using phenotypic high content screening, we present

the biological evaluation of these compounds using an assay detecting the induction of mitotic arrest. We present one hit series, which induces mitotic arrest by depolymerising microtubules and binds in a site vicinal or allosteric to Colchicine.

RESULTS

Library Synthesis

To synthesize the library, we developed a reagent-based DOS approach employing rhodium carbenoid chemistry to produce pluripotent substrates, from which a range of structurally diverse small molecules could be regio- and diastereo-selectively synthesized. To this end, we envisaged the use of phenyldiazo ester compounds (**1** and **12**) as highly functionalized substrates from which a structurally complex compound collection could be constructed (Figures 1 and 2). Rhodium catalyzed cyclopropanation of compound **1**, which was obtained according to literature precedent[24], with a range of unsaturated compounds led to the formation of densely functionalized molecular frameworks (Figure 1). Diastereoselective reaction of **1** with terminal alkynes and alkenes provided cyclopropenes and cyclopropanes respectively in good yields and complete diastereocontrol for **4** (Figure 1, pathways a and b)[25]. Cyclopropene **2** allowed further diversification by palladium catalyzed C-H activation, coupling **2** with *p*-nitroiodobenzene using Heck-type reaction conditions to yield **3**[26]. The generation of functionality variants was accomplished by the reaction of **1** with various allenes, affording the corresponding cyclopropanes with exocyclic alkenes (**5-6**), which could be converted to the lactones (**7-8**) *via* iodo-lactonisation[27]. The remaining iodide was then successfully removed by radical de-iodination to give **9** and **10,** completing a subset of the library based on **1**.

Encouraged by the scope of complexity generating methodology accessible *via* rhodium (II) catalyzed carbenoid chemistry, we decided to synthesize the styryl diazoester derivatives **11** and **12**. Davies *et al.* demonstrated the ability of **11** to undergo tandem cyclopropanation-Cope rearrangement reactions, resulting in the diastereoselective formation of highly functionalized heptadienes[28]. We hypothesized that the synthesis of a bicyclo[3.2.1]octadiene scaffold from a styryl diazoester containing an *ortho*-bromo aryl functionality (as in compound **12),** would furnish a bicyclic construct poised for further diversification. Adorned with reactive functionally, intermediate **12** could be subjected to a variety of diversity generating reactions, thus providing a library of skeletally diverse small molecules containing multiple stereocentres. Taking precedent from the described synthesis of **11,** compound **12** was initially synthesized via a Wittig olefination of bromobenzaldehyde, followed by esterification and diazo formation (Supplementary Figure 1). However, the Wittig reaction provided a mixture of (*E*) and (*Z*) stereoisomers, presumably due to steric hindrance of the bromo substituent. Optimization of the synthetic route followed; treating 2-bromophenyl acetaldehyde with malonic acid in Hünigs base provided the Knoevenagel condensation product. Subsequent esterification delivered a mixture of regioisomers (Supplementary Scheme S1b), which was readily converted to the desired diazo compound **12** as a single (*E*) stereo- and regioisomer.

Intermediate **12** was subjected to a cyclopropanation-Cope rearrangement according to the procedure developed by Davies *et al.* to provide the highly functionalized key intermediate **14** in good yield (Figure 2)[28]. This reaction delivered three new stereocentres with complete diastereocontrol, thereby enabling further diversification via stereocontrolled reactions. The presence of both an electron deficient and an electron neutral olefin in the bicyclic system, coupled with the proximal aryl bromide and a carboxylic acid ester in the backbone of compound **14,** afforded the opportunity to regioselectively modify the scaffold in a multi-directional approach. Our exploration of the chemical space around scaffold **14** began with a stereoselective epoxidation reaction, resulting in the formation of epoxide **15** on the less hindered face in excellent yield. The relative stereochemistry of this compound was confirmed by NOESY experiments, which showed no interaction between the methine epoxide protons and those of the fused ring bridgehead. Regio- and stereoselective dihydroxylation of the electron neutral alkene was performed under Upjohn conditions, using osmium tetroxide, thereby providing the chiral *cis*-diol **16**, containing 5 contiguous stereocentres, and a further molecular construct poised for diversification. The stereochemical relationship of the two new sterocentres confirmed that the dihydroxylation reaction occurs selectively from the less hindered face of heptadiene **14**. Reacting diol **16**, with commercial aldehydes and ketones under acidic conditions provided acetals **17-21**, in good yield. Finally, sulfoxide **22**, which comprises six chiral centres was readily synthesized as a 3:1 mixture of diastereomers, by reacting **16** with thionyl chloride.

The production of new ring systems was achieved by subjecting **14** to one-pot dihydroxylation and oxidative cleavage methodology developed by Nicolaou[29] using (diacetoxyiodo)benzene, followed by reductive amination conditions. The use of dimethylamine enables the synthesis of the highly functionalized cyclohexene **23**, however more interesting heterocyclic scaffolds were accessed when primary amines were utilized, as a consequence of double reductive amination reactions. Thus 6-6 fused ring frameworks, with varied appendage diversity were obtained (Figure 2, compounds **24-31**). We observed that the reducing agent sodium triacetoxyborohydride was essential for this process, to selectively reduce the imines formed in the reaction in

the presence of the aldehyde functionality. The crystal structure of **31** confirmed the expected relative stereochemistry, which had been maintained throughout this three-step, one-pot process. To further increase the diversity of the library, the dialdehyde obtained *via* the dihydroxylation/oxidative cleavage of **14** described above, was selectively reduced to the corresponding diol and spontaneously cyclized through a ring closing transesterification reaction, yielding the novel lactone scaffold **32** in just one synthetic step.

Building block **14** was viewed as a perfect substrate for molecular decoration and adornment in transition metal catalyzed reactions. The electron neutral alkene was amenable to ring opening/cross metathesis (ROCM) with terminal olefins, providing newly functionalized cyclohexene structures **33-35**. On the other hand, the *ortho*-bromo aryl substituent present in **14** provided a functional handle for cross-coupling reactions, introducing appendage diversity around the core scaffold. A series of Suzuki couplings to form new biaryl bonds were also performed. Although the yields for this process were poor, predominantly due to proto-debromination and the formation of compound **13**, sufficient material for biological evaluation was in hand, so we decided to forgo optimization of this process at that stage. In total a library of 35 compounds with 10 distinct molecular scaffolds was synthesized (Supplementary Figure 2), comprising complex fused ring systems of varying size and a multiplicity of stereocenters.

Cheminformatic Analysis

To computationally assess its structural diversity, we carried out a comparative statistical analysis of a set of molecular descriptors for our DOS library and two reference compound collections, comprising 40 top-selling brand-name drugs and 60 diverse natural products[30,31]. Principle component analysis (PCA) utilizes a defined set of molecular descriptors, such as physicochemical properties, to represent each component compound as a vector in n-dimensional space. n-Dimensional vectors can then be reduced to 2-dimensional vectors by an orthogonal transformation, and re-plotted as a scatter plot, thereby providing an illustrative representation of the diversity of the compound collection. Fifteen physicochemical properties (Supplementary Table 1) of the compounds were analyzed using the molecular operating environment (MOE) software. The first three principal components account for 87% of the dataset variance and are represented in 2D plots (Figures 3a-c and Supplementary Table 2). As seen in Figures 3a-c, our DOS library overlaps considerably with the chemical space explored by the top-selling drugs, indicating the potential drug-likeness of the library and possibly intimating that it should access biologically relevant areas of chemical space. Examination of the component loadings (Supplementary Table 3) shows that increases in ring count and number of nitrogen and oxygen atoms shift molecules in the positive direction along the PC1 axes, whereas molecules with high hydrophobicity and ring count are driven in the positive direction along the PC2 axes. Important contributors to the variance in PC3 are nitrogen atom, aromatic atom and ring count, all of which an increase leads to a positive shift along the PC3 axes. These suggest that ring count is an important property contributing to the overlap between our DOS compounds and the drug library.

We also compared the degree of shape diversity in our DOS library with the two reference sets of compounds. Based on the lowest-energy conformations of the compounds, normalized ratios of principal moment of inertia (PMI) were calculated and plotted on a triangular graph[32]. The PMI plot obtained (Figure 3d) illustrates the shape diversity of the compounds, with its vertices representing the three extremes of molecular shape (rod, disc and sphere). The drug reference set predominantly contains rod-like shapes with some disc-like character while the natural products exhibit considerably higher shape diversity. A very good level of shape diversity was achieved by the DOS library. We performed a Kolmogorov-Smirnov test to evaluate whether there is a significant difference between the distances of the vertices to the drugs and DOS library compounds on the PMI plot[33]. The results are not significant for distances to the disc corner ($p = 0.217$). However, the two libraries are significantly different in terms of distances to the other two canonical PMI shapes, with the drugs tending towards the rod corner ($p = 0.027$) and the DOS compounds tending towards the spherical corner ($p = 0.002$). This suggests that the DOS compounds contain scaffolds that are drug-like but are more spherical and 3-dimensional in character than the drugs. This is particularly important, as the lack of 3-dimensionality and low sp^3 carbon content is considered to be one of the main reasons why combinatorial screening collections fail to deliver hits against challenging targets such as protein-protein interactions (PPIs) or protein-DNA interactions[34].

Biological Evaluation

Anti-mitotic compounds are already used clinically, and this target class still holds great promise for anti-cancer therapy. However resistance and administration problems have increased the requirement for new therapies[22, 23]. One avenue to identify anti-mitotic compound is by conducting a phenotypic screen for mitotic arrest. Therefore we focused our attention on a high content screen using automated microscopy[35, 36]. The screen was performed using U2OS osteosarcoma cells, which were incubated for 20 hours with all of the library compounds, stained for the mitotic marker phospho-Histone H3 and imaged on a Cellomics Arrayscan high content microscope. Image analysis allowed us to detect the percentage of cells arrested in mitosis following compound treatment. The assay utilized nocodazole as a positive control and had a Z factor of 0.77, indicating an excellent assay,

particularly for a phenotypic screen (Supplementary Figure 3)[37]. All compounds were soluble at the assay concentration (50 μM) and most compounds re-screened were soluble up to 100 μM. It was encouraging to see that two molecules (**37** and **38**) from the original library showed mitotic arrest, with EC_{50} values in the single-digit micromolar range (Table 1). This is particularly significant as the library was not biased towards a particular type of target class. An additional advantage of the high content screening approach is that one is able to identify compounds that perturb cell function without affecting the primary assay read-out. For example, we were able to identify two compounds (**24** and **26**) that caused a decrease in cell viability with GI_{50}'s of 21 and 14 μM respectively (Supplementary Figure 4) which did not induce a mitotic arrest. Whilst we do not know the targets of these molecules, their identification is a further testament to the ability of DOS to produce potentially useful scaffolds.

Analogue Synthesis

In the mitotic index assay, the most potent compound (**38**) from the primary screen gave a large (35-40%) mitotic arrest, which resulted in tumor cell death in a 72-hour cell viability assay (Table 1). Encouraged by this promising result, we sought a synthetic route that was higher yielding for analogue synthesis. It was envisaged that reducing the electron neutral double bond would reduce the risk of side reactions in the subsequent Suzuki coupling. Moreover, biological evaluation of the reduced products would provide some structural-activity relationship information about the chemotype as well as reduce the possibility of further biochemical reactions. A new synthetic route to the reduced products was devised (Figure 4) to achieve the desired cycloheptene. Diimide reduction of intermediate **14** followed by Suzuki coupling with the appropriate boronic acids provided the desired compounds **40** and **41** in good yield. Both analogues gave a mitotic arrest in U2OS cells. In fact, comparing compound **38** with its partially saturated analogue **41** we observed a two-fold increase in potency. Treatment with **40** and **41** also resulted in growth inhibition in the low micromolar range over a period of 72 hours (Table 1). Given that all compounds were produced as racemates, we predicted that the anti-mitotic activity was likely to reside in just one of the enantiomers. Separation of both enantiomers of Dosabulin by preparative chiral HPLC and subsequent re-testing, revealed that all the activity resided in the *(1R,4S,5S)*-enantiomer, which will henceforth be referred to as *(S)*-**41** (Table 1 and Figure 5a, b, and c). In fact, this enabled the use of the *(1S,4R,5R)*- enantiomer *(R)*-**41** as a negative control. We were then able to show that *(S)*-**41** treated cells died through apoptosis (Supplementary Figure S5)[38] whilst cells treated with *(R)*-**41** did not. At this stage we focused our attention on identifying the mechanism of action of these compounds.

Target Identification

Identification of the targets from a phenotypic screen can often be the rate-limiting step[39]. However, careful observation of the phenotype may sometimes offer clues on what the target may be, allowing more informed experiments to be conducted[40]. Confocal microscopy was used to look at the key mitotic protein, tubulin, for this purpose. This revealed that the tubulin network was heavily disrupted upon treatment with *(S)*-**41** compared to the DMSO control, which suggested that the compound may be targeting tubulin itself (Figure 6a, Supplementary Figure 6). This phenotype was recapitulated by nocodazole, a known tubulin depolymerizer. This result was not altogether unexpected, given that several clinically used anti-mitotics target tubulin polymerization dynamics[41]. Using an *in vitro* tubulin polymerization assay it was established that *(S)*-**41** acts as a tubulin depolymerizing agent,[42] similar to our positive control nocodazole (Figure 6b). This compound was subsequently termed 'Dosabulin', for DOS tubulin inhibitor. The inactive *(R)*-enantiomer did not show any tubulin depolymerization ability. It is widely accepted that several small molecule binding sites exist on tubulin[43]. For example, Vinblastine binds the β-tubulin subunit, whilst Colchicine binds at the α/β interface. Additional compounds targeting tubulin dynamics exist, for which the binding site has yet to be fully elucidated, such as Noscapine and Peloruside. To establish whether *(S)*-Dosabulin bound in either of the established tubulin binding sites which cause depolymerisation, two *in vitro* fluorescence based assays monitoring displacement of Colchicine or Vinblastine from tubulin by *(S)*-Dosabulin were used (Figure 6c and d). To monitor binding at the Vinblastine site, a fluorescence polarization (FP) assay was developed. Using commercially available fluorescently tagged Vinblastine it was shown that polarization increases upon tubulin binding (Supplementary Figure 7). Once the optimal tubulin concentration for a sufficiently large assay window was selected, *(S)*-Dosabulin was screened for its ability to inhibit tubulin at this site. *(S)*-Dosabulin did not significantly affect the binding of fluorescently labeled Vinblastine to tubulin in this FP assay (Figure 6c and Supplementary Figure 8). To determine whether *(S)*-Dosabulin was able to bind in the Colchicine site, the change in intrinsic Colchicine fluorescence when bound to tubulin was measured. A time course experiment as carried out to observe whether *(S)*-Dosabulin was able to displace Colchicine from tubulin (Supplementary Figure 9). In fact, treatment with *(S)*-Dosabulin resulted in a time- and dose-dependent inhibition. However, incomplete inhibition was seen compared to Nocodazole (Figure 6d). This suggests that *(S)*-Dosabulin may not directly displace Colchicine, but rather bind to a site vicinal or allosteric to it, resulting in a decrease of its binding affinity for tubulin.

DISCUSSION

In this study we report the synthesis and biological evaluation of a DOS library constructed using rhodium (II) catalyzed carbenoid chemistry to access key pluripotent intermediates. A total of 35 complex and structurally diverse compounds were synthesized. Biological screening of this collection in a high content microscopy-based approach revealed two compounds that arrested cells in mitosis. Following some structural modifications we identified Dosabulin, a novel small molecule that arrested cells in mitosis by depolymerizing microtubules. It causes a dose-dependent displacement of Colchicine from tubulin, however no complete disruption of the interaction is observed. This suggests that it binds in a site in the vicinity of, or allosteric to Colchicine. *(S)*-Dosabulin causes cell death by apoptosis in U2oS osteosarcoma cells at sub-micromolar concentrations. With new tubulin binding compounds such as eribulin recently being approved[44], and existing therapies suffering from administration and resistance problems[22], new anti-mitotics targeting tubulin are required[23]. We hope that Dosabulin and related studies may spur new drug discovery efforts in this field. To further assess the utility of this library, further biological screens for antibacterial activity and inhibition of selected protein-protein interactions are ongoing. This work validates DOS in combination with phenotypic screening as an effective strategy for the identification of new biologically relevant chemical entities. Adoption of this approach on a wide scale is likely to prove fruitful in the context of chemical genetics and drug discovery.

METHODS

Chemical Synthesis

Compounds were synthesized according to procedures specified in Supplementary Note 1 and Supplementary Methods. X-ray crystallographic data and images are reported in Supplementary Figures 10-12 and Supplementary Tables 1-13. For ^{1}H and ^{13}C NMR spectra of compounds reported see Supplementary Figures 13-45.

Principal component analysis

Principal component analysis (PCA) was carried out using the Molecular Operating Environment (MOE) software package[45]. A total of 15 physicochemical properties (Supplementary Table 14) were obtained for established reference sets of 40 top-selling brand-name drugs and 60 diverse natural products and 36 DOS library members[30]. The summary of the contribution of each principal component is shown in Supplementary Table 15 and the component loadings are shown in Supplementary Table 16. The first three principal components account for 86.9 % of the variance in the dataset and were used to generate Figure 3a-c.

Principal moment of inertia calculations

We compared the molecular shape diversity of our DOS library with the reference sets of 100 compounds used in the PCA. The stochastic conformational search algorithm in the MOE software package was used to generate 3D conformers for each compound. The MMFF94x force field was used with the generalized Born solvation model for the minimizations. Sampling and minimization parameters were implemented as follows:

Stochastic Search Limit: 7
Refinement Conformation Limit: 300
Stochastic Search Failure Limit: 100
Stochastic Search Iteration Limit: 1000
Energy Minimization Iteration Limit: 200
Energy Minimization Gradient Test: 0.01

Only the conformer with the lowest energy was retained for principal moment of inertia (PMI) calculations in each conformational sampling run. Normalized PMI ratios (I_1/I_3 and I_2/I_3) of these conformers were obtained from MOE and then plotted on a triangular graph, with the coordinates (0,1), (0.5,0.5) and (1,1) representing a perfect rod, disc and sphere respectively (Figure 3d).

High Content Analysis – Mitotic Index

HCA was performed using an Arrayscan II HCS reader and integrated software from Cellomics. U2oS osteosarcoma cells (ATCC) were seeded in a NUNC clear flat-bottomed 96-well plate at 10,000/well in a total of 100 μL. They were incubated at 37 ºC overnight. Cells were then treated with compounds (25 μL) to give the appropriate concentration. Cells were then incubated at 37 ºC for 20 h. 50 μL 12.5 % formaldehyde was added to each well. This was incubated at RT for 10 min, before the formaldehyde was gently removed. 100 μL/well permeabilization buffer (PB, contains PBS + 0.1% Triton X-100), was then added to each well, incubating for 10 min. PB was removed and wells were washed with 100 μL/well blocking buffer (BB, contains PBS + 1%

BSA). BB was removed and 50 µL/well of primary antibody solution (anti-pH3 (S10), Abcam, ab5176, 1:2000) was added. Plates were incubated for 1 h at room temperature. The antibody was removed and wells washed with 2 x 100 µL/well BB. BB was removed and 50 µL/well of secondary antibody solution containing Hoechst (Invitrogen, H3570, 1:2500) and AlexaFluor 488 Goat anti-rabbit IgG (Invitrogen, A11034) was added. Plates were incubated at RT for 1 h in the dark. Secondary antibody solution was removed and plates washed with 2 x 100 µL BB. The BB was then removed and 100 µL PBS/well were added. The plates were sealed with opaque film and images taken on a 20x 0.4 NA objective. Data was analysed on Cellomics Arrayscan software using the Target Activation v4 protocol. Critical output features are: ValidObjectCount and %Responder_AvgIntenCh2. EC_{50} data was calculated using Prism (Graphpad) and is an average of three independent experiments conducted in triplicate.

Sulforhodamine B colorimetric assay for cytotoxicity screening

This assay was conducted according to literarure procedure[46]. U2oS cells were seeded at 4000 cells/well in 180 µL and incubated for 20 h at 37 °C. Compounds were then added in 20 µL to give the desired concentrations. After incubation for 72 h at 37 °C the medium was removed by aspiration, and 100 µL of 1% TCA solution was added. This was incubated for 1 h and then removed. The plates were washed 4 x with tap water and the plates were allowed to air dry at RT. 100 µL of a 0.057 % wt/vol solution of Sulforhodamine B (Sigma Aldrich) were added to each well, incubating for 30 min. The plates were then washed quickly with 4 x 100 µL of acetic acid solution (1%) and then air-dried. 200 µL of TRIS buffer (10 mM, pH 8.0) was added to each well to resolubilise the dye. The plates were then read at 510 nm on a Infinite® M200 plate reader (Tecan, Austria). GI_{50} data was calculated using Prism (Graphpad) and is an average of three independent experiments conducted in triplicate.

Confocal Microscopy

200,000 U2oS cells were seeded on coverslips in 2 mL medium in a six-well plate and incubated at 37 °C overnight. Compounds were added in DMSO to the appropriate concentration and the cells were incubated for 16 hours. The medium was then aspirated and the cells were then fixed in 1 mL PBS containing 4% *para*-formaldehyde for 10 min. Cells were permeabilised in PBS containing 0.1% Triton-X (PBS-T) for 10 min and then washed with 1 mL PBS containing 1% BSA (PBS-BSA). Tubulin was visualized using an α-tubulin antibody (1:1000) in 500 µL for 2 h. The primary antibody was then removed and the cells were washed with 1 mL PBS-BSA three times. Alexafluor-488 conjugated goat anti-rabbit (Invitrogen, A11034) secondary antibody was then added in 500 µL PBS-BSA for 1 h. The secondary antibody was removed and cells were washed twice with PBS-BSA and once with PBS. The coverslips were mounted on slides with mounting medium containing DAPI and imaged on a Zeiss LSM-510 confocal microscope with a 100X objective.

Tubulin *in vitro* polymerization assay

This assay was performed according to the literature procedure[42]. Compounds were dissolved in 10 µL 1X General Tubulin buffer (PEM) containing 80 mM Na-PIPES pH 6.9, 1 mM $MgCl_2$ and 1 mM EGTA and added to wells in a 96-well plate. The tubulin solution was prepared by dissolving porcine α/β-tubulin (> 99% pure, Cytoskeleton, USA) in 1X General Tubulin Buffer containing 10% glycerol, and 1 mM GTP. 100 µL of this tubulin solution (3.0 mg/mL) was added to the compound solutions or the control prewarmed in the 96-well plate at 37 °C. Tubulin polymerization was monitored over 60 min by reading the increase in fluorescence at ex/em 340/460 nm in the Infinite® M200 plate reader (Tecan, Austria).

Colchicine competition assay

3 µM tubulin was incubated with 3 µM colchicine (Sigma Aldrich) and the appropriate concentrations of (S)-Dosabulin or nocodazole in PEM buffer at 37 °C for a total volume of 45 µL/well in black 384-well plates (Corning). Fluorescence readings (ex/em 365/435 nm) were taken every 15 min for 1.5 h using Infinite® M200 plate reader (Tecan, Austria). Fluorescence values were normalized to the DMSO control.

Vinblastine competition assay

Tubulin (2 µM) and BODIPY-FL-vinblastine (2 µM, Invitrogen) in PEM buffer were incubated with different concentrations of (S)-Dosabulin, or vinblastine sulfate (Alfa Aesar) for 20 min at RT in a total volume of 45 µL/well. Fluorescence polarization readings were performed in black 384 well plates using a PHERASTAR plate reader (excitation/emission wavelengths 485/520 nm). FP values were normalized to the DMSO control.

Accession Codes

The X-ray crystallographic coordinates for structures reported in this Article have been deposited at the Cambridge Crystallographic Data Centre (CCDC), under deposition numbers CCDC 936205, 936206, and 936208. These data can be obtained free of charge from The Cambridge Crystallographic Data Centre via www.ccdc.cam.ac.uk/data_request/cif.

REFERENCES

1. O' Connor CJ, Beckmann HSG, Spring DR. Diversity-oriented synthesis: producing chemical tools for dissecting biology. *Chem. Soc. Rev.* **41**, 4444-4456 (2012).
2. Tan DS. Diversity-oriented synthesis: exploring the intersections between chemistry and biology. *Nat. Chem. Biol.* **1**, 74-84 (2005).
3. Galloway WRJD, Isidro-Llobet A, Spring DR. Diversity-oriented synthesis as a tool for the discovery of novel biologically active small molecules. *Nat. Commun.* **1**, 80 (2010).
4. Ascic E, Jensen JF, Nielsen TE. Synthesis of Heterocycles through a Ruthenium-Catalyzed Tandem Ring-Closing Metathesis/Isomerization/N-Acyliminium Cyclization Sequence. *Angew. Chem. Int. Ed.* **50**, 5188-5191 (2011).
5. Huigens III RW, Morrison KC, Hicklin RW, Flood Jr TA, Richter MF, Hergenrother PJ. A ring-distortion strategy to construct stereochemically complex and structurally diverse compounds from natural products. *Nat. Chem.* **5**, 195-202 (2013).
6. Davies HML, Morton D. Guiding principles for site selective and stereoselective intermolecular C-H functionalization by donor/acceptor rhodium carbenes. *Chem. Soc. Rev.* **40**, 1857-1869 (2011).
7. Wu J, Becerril J, Lian Y, Davies HML, Porco JA, Panek JS. Sequential Transformations to Access Polycyclic Chemotypes: Asymmetric Crotylation and Metal Carbenoid Reactions. *Angew. Chem. Int. Ed.* **50**, 5938-5942 (2011).
8. Clemons PA, *et al.* Quantifying structure and performance diversity for sets of small molecules comprising small-molecule screening collections. *Proc. Natl. Acad. Sci.* **108**, 6817-6822 (2011).
9. Luker T, *et al.* Strategies to improve in vivo toxicology outcomes for basic candidate drug molecules. *Bioorg. Med. Chem. Lett.* **21**, 5673-5679 (2011).
10. Ritchie TJ, Macdonald SJF. The impact of aromatic ring count on compound developability,Äìare too many aromatic rings a liability in drug design? *Drug Discov. Today* **14**, 1011-1020 (2009).
11. O' Connor CJ, Laraia L, Spring DR. Chemical genetics. *Chem. Soc. Rev.* **40**, 4332-4345 (2011).
12. Swinney DC, Anthony J. How were new medicines discovered? *Nat. Rev. Drug. Discov.* **10**, 507-519 (2011).
13. Oh S, Park SB. A design strategy for drug-like polyheterocycles with privileged substructures for discovery of specific small-molecule modulators. *Chem. Commun.* **47**, 12754-12761 (2011).
14. Thomas GL, *et al.* Anti-MRSA agent discovery using diversity-oriented synthesis. *Angew. Chem. Int. Ed.* **47**, 2808-2812 (2008).
15. Stanton BZ, *et al.* A small molecule that binds Hedgehog and blocks its signaling in human cells. *Nat. Chem. Biol.* **5**, 154-156 (2009).
16. Heidebrecht RW, *et al.* Diversity-Oriented Synthesis Yields a Novel Lead for the Treatment of Malaria. *ACS Med. Chem. Lett.* **3**, 112-117 (2012).
17. Wetzel S, Bon RS, Kumar K, Waldmann H. Biology-Oriented Synthesis. *Angew. Chem. Int. Ed.* **50**, 10800-10826 (2011).
18. Antonchick AP, *et al.* Highly enantioselective synthesis and cellular evaluation of spirooxindoles inspired by natural products. *Nat. Chem.* **2**, 735-740 (2010).
19. Dueckert H, *et al.* Natural product inspired cascade synthesis yields modulators of centrosome integrity. *Nat. Chem. Biol.* **8**, 179-184 (2011).
20. Mayer TU, Kapoor TM, Haggarty SJ, King RW, Schreiber SL, Mitchison TJ. Small Molecule Inhibitor of Mitotic Spindle Bipolarity Identified in a Phenotype-Based Screen. *Science* **286**, 971-974 (1999).
21. Mitchison TJ. Small-Molecule Screening and Profiling by Using Automated Microscopy. *ChemBioChem* **6**, 33-39 (2005).
22. Kavallaris M. Microtubules and resistance to tubulin-binding agents. *Nat. Rev. Cancer* **10**, 194-204 (2010).
23. Dumontet C, Jordan MA. Microtubule-binding agents: a dynamic field of cancer therapeutics. *Nat. Rev. Drug Discov.* **9**, 790-803 (2010).
24. Yu W-Y, Tsoi Y-T, Zhou Z, Chan ASC. Palladium-Catalyzed Cross Coupling Reaction of Benzyl Bromides with Diazoesters for Stereoselective Synthesis of (E)-α,β-Diarylacrylates. *Org. Lett.* **11**, 469-472 (2008).
25. Liao L-a, Zhang F, Yan N, Golen JA, Fox JM. An efficient and general method for resolving cyclopropene carboxylic acids. *Tetrahedron* **60**, 1803-1816 (2004).
26. Chuprakov S, Rubin M, Gevorgyan V. Direct Palladium-Catalyzed Arylation of Cyclopropenes. *J. Am. Chem. Soc.* **127**, 3714-3715 (2005).
27. Ma S, Lu L. An Efficient Stereoselective Synthesis of 4,5-trans-1,5-cis-3-Oxabicyclo[3.1.0]hexan-2-

ones via the Iodolactonization of Alkylidenecyclopropyl Esters. *J. Org. Chem.* **70**, 7629-7633 (2005).
28. Davies HML, Stafford DG, Doan BD, Houser JH. Tandem Asymmetric Cyclopropanation/Cope Rearrangement. A Highly Diastereoselective and Enantioselective Method for the Construction of 1,4-Cycloheptadienes. *J. Am. Chem. Soc.* **120**, 3326-3331 (1998).
29. Nicolaou KC, Adsool VA, Hale CRH. An Expedient Procedure for the Oxidative Cleavage of Olefinic Bonds with $PhI(OAc)_2$, NMO, and Catalytic OsO_4. *Org. Lett.* **12**, 1552-1555 (2010).
30. Bauer RA, Wurst JM, Tan DS. Expanding the range of 'druggable' targets with natural product-based libraries: an academic perspective. *Curr. Opin. Chem. Biol.* **14**, 308-314 (2010).
31. Kopp F, Stratton CF, Akella LB, Tan DS. Diversity-Oriented Synthesis Approach to Macrocycles via Oxidative Ring Expansion. *Nat. Chem. Biol.* **8**, 358 (2012).
32. Sauer WHB, Schwarz MK. Molecular Shape Diversity of Combinatorial Libraries: A Prerequisite for Broad Bioactivity. *J. Chem. Inf. Comput. Sci.* **43**, 987-1003 (2003).
33. Hung AW, *et al.* Route to three-dimensional fragments using diversity-oriented synthesis. *Proc. Natl. Acad. Sci. USA* **108**, 6799-6804 (2011).
34. Lovering F, Bikker J, Humblet C. Escape from Flatland: Increasing Saturation as an Approach to Improving Clinical Success. *J. Med. Chem.* **52**, 6752-6756 (2009).
35. O'Connell KMG, *et al.* A two-directional strategy for the diversity-oriented synthesis of macrocyclic scaffolds. *Org. Biomol. Chem.* **10**, 7545-7551 (2012).
36. Young DW, *et al.* Integrating high-content screening and ligand-target prediction to identify mechanism of action. *Nat. Chem. Biol.* **4**, 59-68 (2008).
37. Zhang JH, Chung TD, Oldenburg KR. A Simple Statistical Parameter for Use in Evaluation and Validation of High Throughput Screening Assays. *J. Biomol. Screen.* **4**, 67-73 (1999).
38. Zheng S, *et al.* Synthesis and biological profiling of tellimagrandin I and analogues reveals that the medium ring can significantly modulate biological activity. *Org. Biomol. Chem.* **10**, 2590-2593 (2012).
39. Ziegler S, Pries V, Hedberg C, Waldmann H. Target Identification for Small Bioactive Molecules: Finding the Needle in the Haystack. *Angew. Chem. Int. Ed.* **52**, 2744-2792 (2013).
40. Neumann B, *et al.* Phenotypic profiling of the human genome by time-lapse microscopy reveals cell division genes. *Nature* **464**, 721-727 (2010).
41. Stanton RA, Gernert KM, Nettles JH, Aneja R. Drugs that target dynamic microtubules: A new molecular perspective. *Med. Res. Rev.* **31**, 443-481 (2011).
42. Voigt T, *et al.* A Natural Product Inspired Tetrahydropyran Collection Yields Mitosis Modulators that Synergistically Target CSE1L and Tubulin. *Angew. Chem. Int. Ed.* **52**, 410-414 (2013).
43. Gigant B, *et al.* Structural basis for the regulation of tubulin by vinblastine. *Nature* **435**, 519-522 (2005).
44. Cortes J, *et al.* Eribulin monotherapy versus treatment of physician's choice in patients with metastatic breast cancer (EMBRACE): a phase 3 open-label randomised study. *The Lancet* **377**, 914-923 (2011).
45. Inc., C.C.G. Molecular Operating Environment (MOE). 2011.10 edn (1010 Sherbooke St. West, Suite #910, Montreal, QC, Canada, H3A 2R7, 2011).
46. Vichai V, Kirtikara K. Sulforhodamine B colorimetric assay for cytotoxicity screening. *Nat. Protocols* **1**, 1112-1116 (2006).

Acknowledgements
The authors would like to thank Amy Emery for help with confocal microscopy, and Dr. John Davies for crystallographic assistance. We would also like to thank the EU, ERC, EPSRC, Cancer Research UK, BBSRC, MRC, Wellcome Trust, A*STAR and the Frances and Augustus Newman foundation for funding.

Author Contribution B.M.I, L.L, G.J.M, A.R.V, and D.R.S designed experiments. B.M.I. and E.A. synthesized the DOS library, L.L. conducted the phenotypic screen, biological validation and target identification, and synthesized analogues. G.J.M. assisted with data analysis. Y.S.T. conducted the cheminformatics analysis. H.M.L.D. provided key reagents. L.L. wrote the paper with assistance from E.A, C.O, G.J.M, A.R.V. and D.R.S.

Conflict of interest statement
The authors declare no competing financial interests.

Supplementary information and chemical compound information accompanies this paper at http://www.nature.com/naturecommunications

Competing Financial Interests: The authors declare no competing financial interests.

How to cite this article

FIGURES

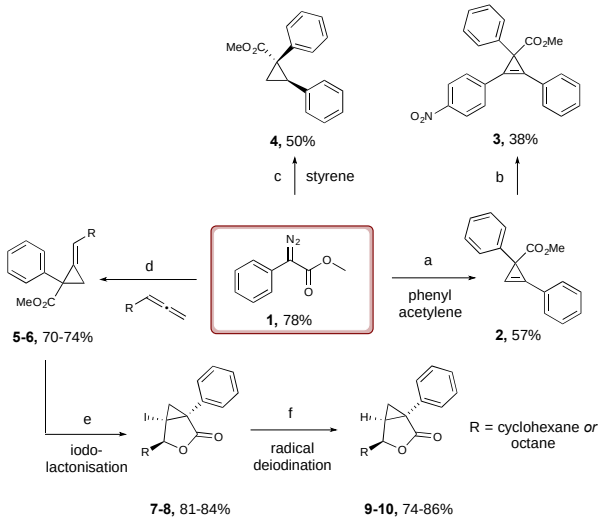

Figure 1. Synthetic scheme of DOS library subset based on **1**; (a) Phenylacetylene, $Rh_2(OAc)_4$ (1 mol%), CH_2Cl_2; (b) *p*-nitroiodobenzene, $Pd(OAc)_2$ (10 mol%), K_2CO_3, DMF; (c) styrene, $Rh_2(OAc)_4$ (1 mol%), CH_2Cl_2; (d) undeca1,2diene *or* propa-1,2-dien-1-ylcyclohexane, $Rh_2(OAc)_4$ (1 mol%), CH_2Cl_2; (e) *N*-iodosuccinimide, MeCN-H_2O (2:1), 50 °C; (f) Bu_3SnH, AIBN, PhH, 80 °C;

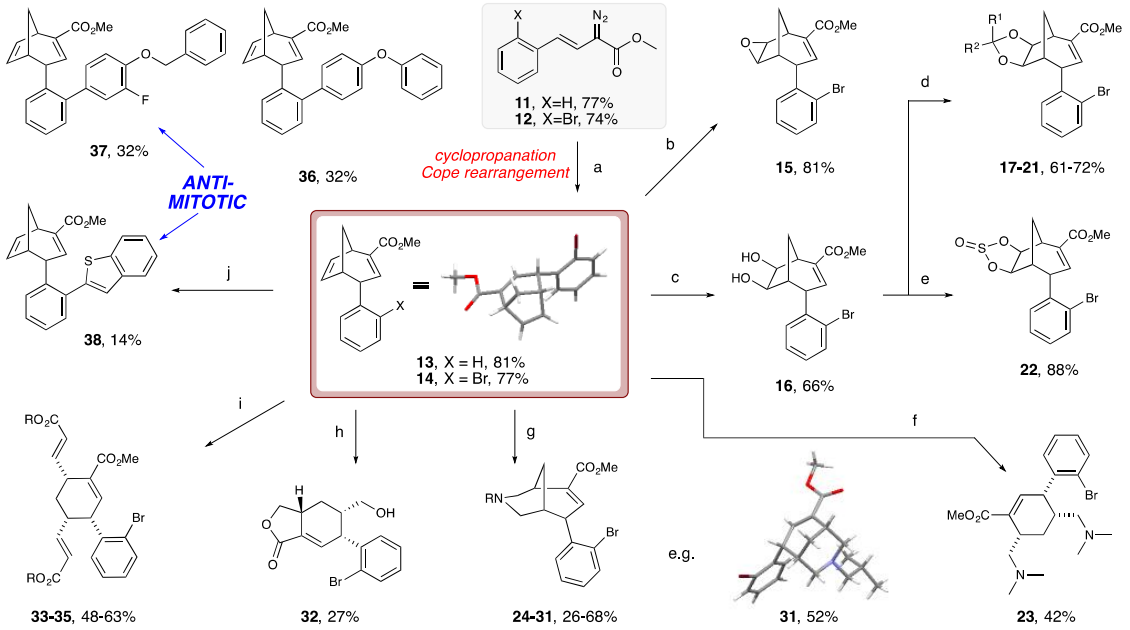

Figure 2. Library synthesis from key building block **14**; (a) cyclopentadiene, $Rh_2(OAc)_4$ (1 mol%), CH_2Cl_2; (b) *m*-CPBA, CH_2Cl_2; (c) OsO_4 (2.5 mol%), NMO, acetone-H_2O (9:1); (d) aldehyde/ketone, CSA (10 mol%), 3Å molecular sieves, CH_2Cl_2; (e) $SOCl_2$, CH_2Cl_2; (f) 2,6-lutidine, NMO, OsO_4 (2.5 mol%), $PhI(OAc)_2$, acetone-H_2O (10:1), then dimethylamine, $NaBH(OAc)_3$, CH_2Cl_2; (g) 2,6-lutidine, NMO, OsO_4 (2.5 mol%), $PhI(OAc)_2$, acetone-H_2O (10:1), then primary amine, $NaBH(OAc)_3$, CH_2Cl_2; (h) 2,6-lutidine, NMO, OsO_4 (2.5 mol%), $PhI(OAc)_2$, acetone-H_2O (10:1), then $NaBH_4$, MeOH; (i) alkene, Hoveyda-Grubbs (II) catalyst (10 mol%), ethylene, PhMe, 100 °C; (j) $Pd(OAc)_2$ (10 mol%), PPh_3 (15 mol%), 2N K_2CO_3, PhMe, 90 °C;

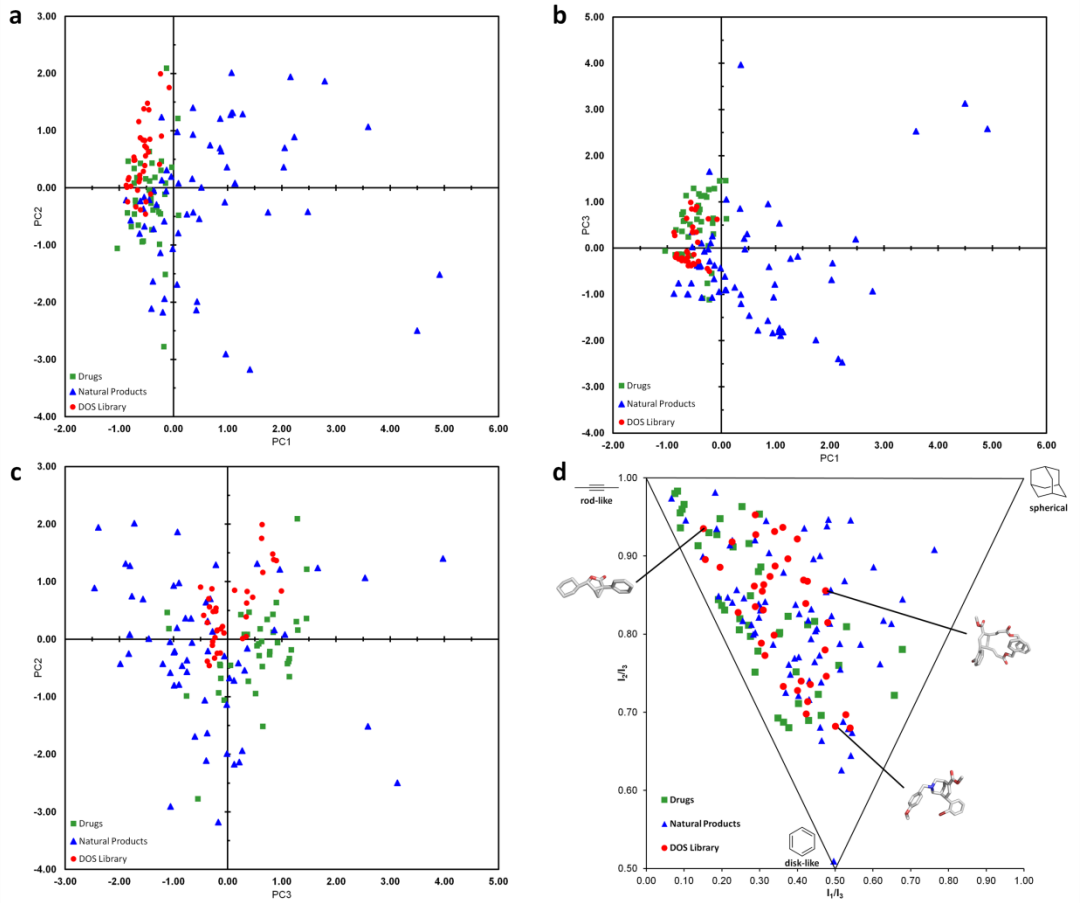

Figure 3. PCA and PMI plots of 35 DOS library compounds (red), 40 top-selling brand-name drugs (green) and 60 diverse natural products (blue); (a) PCA plot of PC1 versus PC2; (b) PCA plot of PC1 versus PC3; (c) PCA plot of PC3 versus PC2; (d) PMI plot illustrating the molecular shape diversity of the DOS library and lowest-energy conformations of three representative DOS library members.

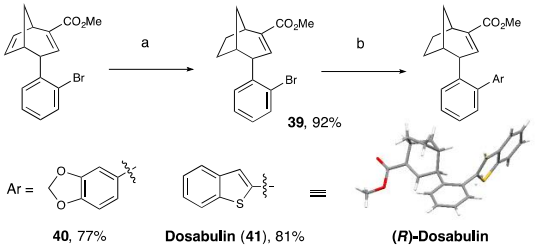

Figure 4. Synthetic route to new analogues of anti-mitotic compounds; (a) $CuCl_2$, hydrazine hydrate, EtOH; (b) $ArB(OH)_2$, $Pd(PPh_3)_4$ (5 mol%), 2N K_2CO_3, dioxane, 120 °C, μW.

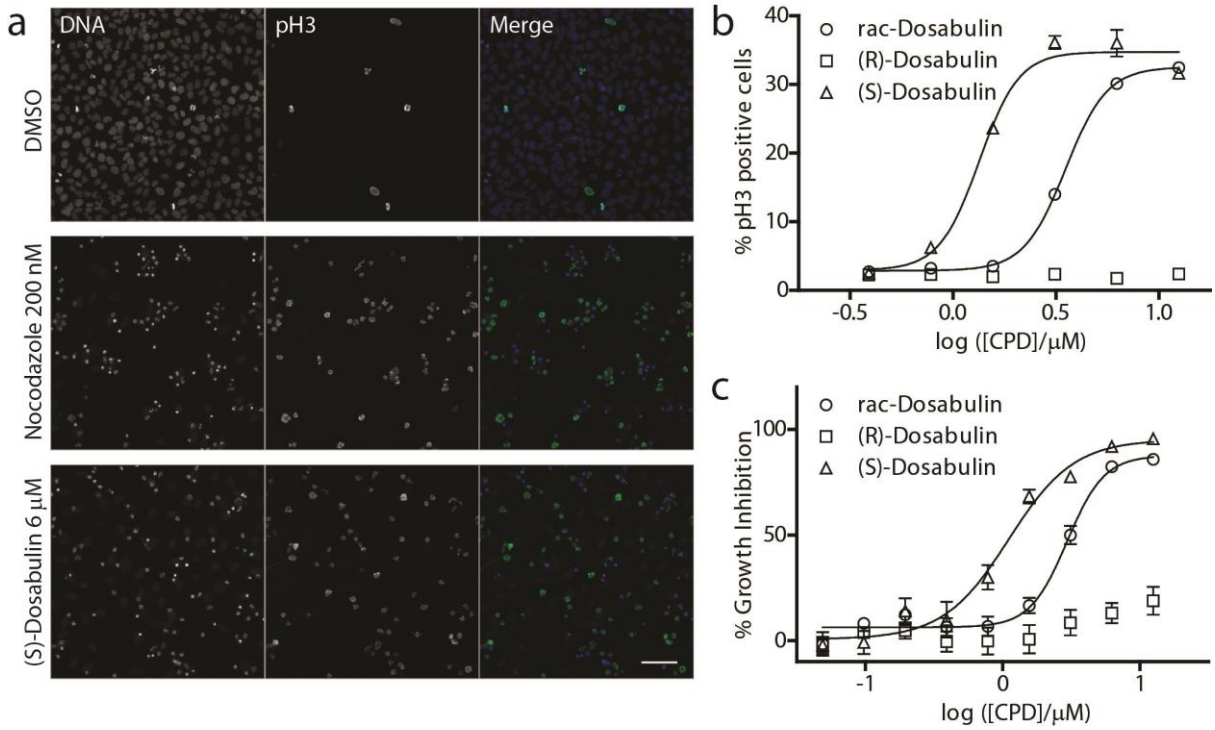

Figure 5. Biological screening results of the DOS library; (a) Representative image output from the phenotypic screen, highlighting the increase in mitotic cells for those treated with the positive control nocodazole and (S)-Dosabulin. U2oS cells were stained with Hoechst (blue) and a phospho-Histone H3 (pH3) antibody (green). Data was collected on a cellomics arrayscan high content microscope with a 20X planfluor objective; scale bar: 70 µm; (b) Representative mitotic index assay data in U2oS cells for racemic Dosabulin and its purified enantiomers. Data points are mean ± s.e.m. of an experiment conducted in triplicate. CPD = compound; (c) Growth inhibition curves in U2oS cells assessed by sulforhodamine B assay for Dosabulin and its purified enantiomers. Cells were treated with compounds for 72 h, before fixing and treating with the protein dye. Data points are mean ± s.e.m. of an experiment conducted in triplicate;

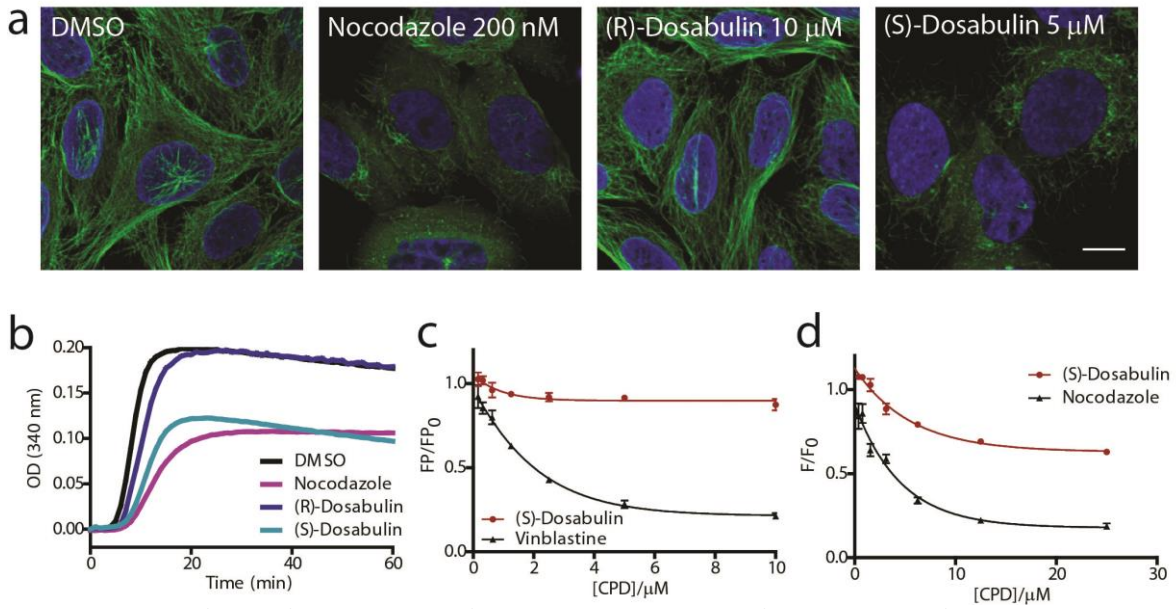

Figure 6. Target identification of Dosabulin: (a) Confocal microscopy in U2oS cells of both enantiomers of Dosabulin show that the (*S*)-enantiomer disrupts the tubulin network in interphase cells, similarly to nocodazole, whilst the (*R*)-enantiomer does not. U2oS cells were stained with DAPI (blue) and an α-tubulin specific antibody (green). Scale bar: 15 µm; (b) *in vitro* tubulin polymerization data shows that (*S*)-Dosabulin causes a decrease in tubulin polymerization, confirming this as a mechanism of action. Porcine brain tubulin (3 mg/mL) kept at 4 °C was incubated with test compounds for 60 min at 37 °C. Compound concentrations: (*S*)-Dosabulin and (*R*)-Dosabulin used at 20 µM, nocodazole at 5 µM. OD = Optical Density; (c) fluorescence polarization (FP) data using FL-BODIPY-Vinblastine (2 µM) as a tracer shows that (*S*)-Dosabulin does not bind tubulin in the Vinblastine site. FP values were normalized to the DMSO control, and data points are mean ± s.e.m. of an experiment conducted in triplicate (ex/em wavelengths 485/520). CPD = compound; (d) fluorescence intensity (F) measurements using Colchicine show that (*S*)-Dosabulin (red) causes a dose-dependent decrease in fluorescence without completely inhibiting the interaction and thus is likely to bind in the vicinity or allosterically to Colchicine. F values were normalized to the DMSO control and data points are mean ± s.e.m. of an experiment conducted in triplicate (ex/em wavelengths 365/435 nm).

Compound Code	Mitotic Index (MI) EC_{50} (µM)	Growth Inhibition $(GI)_{50}$ (µM)
36	N/A	N/A
37	8.90 ± 0.42	4.30 ± 1.13
38	6.25 ± 0.91	3.70 ± 0.71
40	9.48 ± 1.10	4.20 ± 0.62
Dosabulin, 41	3.13 ± 0.32	1.47 ± 0.03
***(R)*-Dosabulin**	N/A	N/A
***(S)*-Dosabulin**	1.23 ± 0.10	0.81 ± 0.37

Table 1. Mitotic arrest EC_{50} and growth inhibition IC_{50} values in U2oS for hit compounds. Data displayed as mean ± S.D, n = 3; N/A = not active.